2014 IEEE International Conference on Robotics & Automation (ICRA)
Hong Kong Convention and Exhibition Center
May 31 - June 7, 2014. Hong Kong, China

Stiffness Analysis of Double Tendon Underactuated Fingers

Bruno Belzile[1] and Lionel Birglen[2]

***Abstract*— Underactuated mechanisms are commonly used in robotic hands and grippers to improve their ability to adapt to the shape of an object. These underactuated mechanisms can be characterized by their global stiffness as measured by their actuator. Using this with self-adaptive fingers, it is possible to elaborate equations highlighting the relationship between the stiffness measurements and the contact locations. In this paper, a complete stiffness analysis of a general double tendon underactuated finger is performed with the aim of establishing the contact locations without any tactile sensors.**

I. INTRODUCTION

Self-adaptive fingers and hands, which are made of an underactuated mechanical system, have the particularity of enabling shape adaptation without complex control algorithms. Many existing robotic hands described in the literature are underactuated and are notably efficient in grasping and manipulation. While they have less actuators than degrees of freedom (DOF), passive elements such as springs are used to constraint their motion. Although there are several differents types of transmission mechanisms existing in underactuated fingers, tendon-driven fingers are very common since they are compact and have an interesting transmission factor of the input force [1], [2], [3], [4].

To provide a tactile feedback, external sensors are generally used. Many efforts have been done recently to improve their performances and make them more efficient in grasping applications [5], [6]. However, they can be expensive and suject to local instabilities such as slippage or other dynamic phenomena. The idea of using other types of sensors has been around for more than two decades. For example, force and torque sensors have been put inside fingertips to collect data from inside the finger and provide a sensory feedback without external sensors. This was referred to as "intrinsic tactile sensing" [7]. Another similar possible solution to collect tactile data is to use measurements provided by proprioceptive (internal) sensors already present. This can be found in the literature as "extended physiological proprioception" [8]. Recently, the idea has been applied to underactuated fingers, including by the authors [9], [10], as it has been done for fully actuated fingers [11]. In this latter case, it was shown that an accurate modeling of the stiffness of the finger was required to obtain reliable tactile data. A similar methodology with proprioceptive sensors can be found in the literature to detect contacts and collisions [12].

[1]Bruno Belzile is with the Department of Mechanical Engineering, Polytechnique Montreal, C.P. 6079, succ. Centre-ville, Montreal, QC H3C 3A7, bruno.belzile@polymtl.ca

[2]Lionel Birglen is with the Department of Mechanical Engineering, Polytechnique Montreal, lionel.birglen@polymtl.ca

In this paper, a complete stiffness analysis of a common type of underactuated finger is performed. Knowing from previous works [9] that the measured global stiffness of an underactuated system depends on the amplitude and location of the contact forces, the objective is to obtain equations in which the contact location is the only unknown variable. It was also shown that tactile sensing based solely on proprioceptive sensors in a compliant gripper is possible even if undesired effects such as hysteresis are present. The stiffness analysis of underactuated fingers can be found in the literature [13], but the focus in this work is placed on the actuation perspective, namely the stiffness of the architecture measured at the actuated joint. Additionally, it is the first time to the best of the authors' knowledge that it is used with the aim of providing tactile feedback. This paper begins with a general presentation of double tendon fingers, followed by the theoretical framework and numerical simulations.

II. TENDON-DRIVEN FINGERS

While many different mechanical designs exist for self-adaptive fingers, tendon-driven fingers are generally the most compact and light. An actuation tendon is used to transmit the driving force and is responsible for the closing motion. Moreover, other mechanical elements are used to constrain the finger and have an opening motion when the actuation force is reduced or eliminated. Commonly, springs or compliant elements are used to this end. With the aim of reducing further the complexity and the mass of the finger, an elastic tendon can also be used [1].

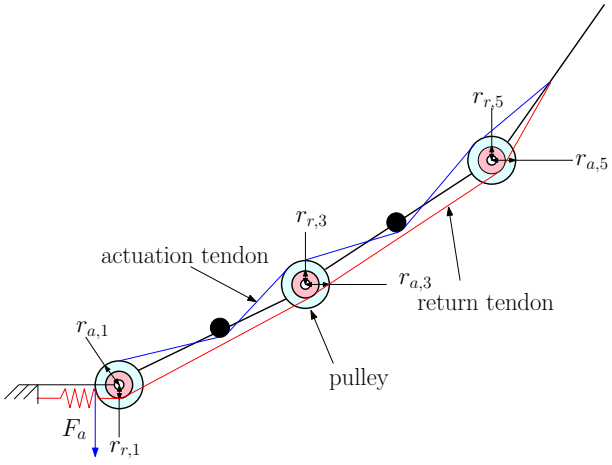

Fig. 1. Finger and tendon routing

Although many tendon routings exist, the one used in this paper and shown in Fig. 1 [14] has been selected for

its relevance for prosthetics. The pulleys in this mechanism are freely rotating and are not coupled with any phalanx. This mechanism can be characterized by a Transmission matrix [15] composed of transmission coefficients X_i, with $i = 1,\ldots,n$ where n is the number of DOF (phalanges) of the finger. To generalize the analysis to other similar types of mechanisms, the general expressions of the transmission coefficients (X_i) are used as much as possible in this work. The geometrical parameters used in numerical simulations are shown in Table I and illustrated in Figs. 1-2. In the latter figure, $\mathbf{f}_i$ and k_i are respectively the contact force on the finger and its distance from the proximal end of the phalanx. The equivalent torques $\boldsymbol{\tau}_a$ and $\boldsymbol{\tau}_r$ transmitted by the tendon mechanism are shown at the interphalanx joints. The torques $\boldsymbol{\tau}_s$ induced by the mechanical limits (if valid) are also shown.

TABLE I

GEOMETRIC PARAMETERS OF A THREE-PHALANX TENDON-DRIVEN FINGER

l_1	45	$r_{r,1}$	2.95
l_2	25	$r_{r,3}$	2.75
l_3	20	$r_{r,5}$	2.00
$r_{a,1}$	6.00	$\theta_{1,0}$	0
$r_{a,3}$	2.75	$\theta_{2,0}$	0
$r_{a,5}$	1.50	$\theta_{3,0}$	0
K_r	10	θ_0	0.1

III. STIFFNESS ANALYSIS

A. Hypotheses

In order to perform a quasi-static analysis of this underactuated finger, it is assumed that the kinetic energy is negligeable compared to the potential energy stored in the return tendon. The effect of gravity is considered negligible compared to the internal forces of the mechanism. Also, the contact on each phalanx is considered to be a single point and the object immovable.

B. Variables

Before continuing with the stiffness analysis, some variables must be defined. The velocity vector $\dot{\boldsymbol{\theta}}$ account for the phalanx velocities. It is defined as:

$$\dot{\boldsymbol{\theta}} = \begin{bmatrix} \dot{\theta}_1 & \dot{\theta}_2 & \ldots & \dot{\theta}_n \end{bmatrix}^T, \tag{1}$$

assuming that the passive elements are located between the phalanges (modeling the effect of the return tendon [14]). Its primitive is $\boldsymbol{\theta}$. Throughout the paper, the indices 0 and i are used to represent the configuration at rest and the instantaneous configuration.

C. Kinetostatics

While it depends on the application, it can be assumed that robotic fingers used to explore unstructured environment do not move very fast, thus making quasi-static analysis an appropriate approach. Assuming this situation, the formulation of the contact forces in self-adaptive fingers is [15]:

$$\mathbf{f} = \mathbf{J}^{-T}\boldsymbol{\tau} = \mathbf{J}^{-T}(\boldsymbol{\tau}_a + \boldsymbol{\tau}_r + \boldsymbol{\tau}_s), \tag{2}$$

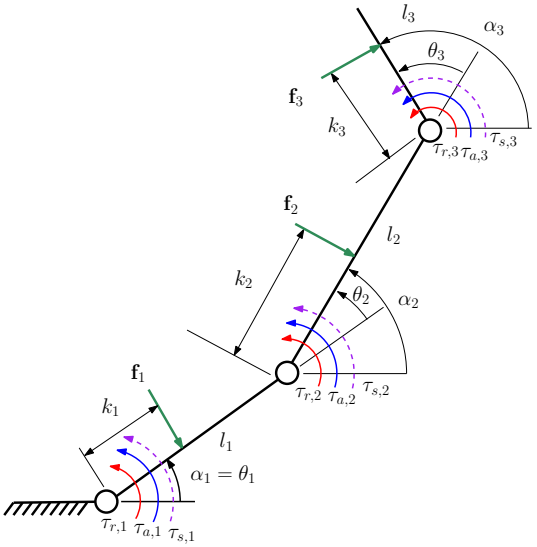

Fig. 2. Geometrical parameter of the finger

where $\mathbf{f} = [f_1 \ldots f_n]^T$ are the normal contact force magnitudes at the phalanges, $\mathbf{J}$ is the Jacobian matrix and $\boldsymbol{\tau}_a$, $\boldsymbol{\tau}_r$, $\boldsymbol{\tau}_s$ are the torques at the interphalanx joints caused respectively by the actuation tendon, the return tendon and the mechanical limits (if required). The actuation torque vector $\boldsymbol{\tau}_a$ and the return torque vector $\boldsymbol{\tau}_r$ are defined as:

$$\boldsymbol{\tau}_a = \begin{bmatrix} 1 & 0 & 0 \\ -X_{a,2} & 1 & 0 \\ -X_{a,3} & 0 & 1 \end{bmatrix} \begin{bmatrix} T_a \\ 0 \\ 0 \end{bmatrix} = \left[\begin{array}{c|cc} \mathbf{x_a} & \mathbf{0}^T \\ \hline & \mathbf{I} \end{array}\right] \begin{bmatrix} T_a \\ 0 \\ 0 \end{bmatrix}, \tag{3}$$

$$\boldsymbol{\tau}_r = \begin{bmatrix} 1 & 0 & 0 \\ -X_{r,2} & 1 & 0 \\ -X_{r,3} & 0 & 1 \end{bmatrix} \begin{bmatrix} T_r \\ 0 \\ 0 \end{bmatrix} = \left[\begin{array}{c|cc} \mathbf{x_r} & \mathbf{0}^T \\ \hline & \mathbf{I} \end{array}\right] \begin{bmatrix} T_r \\ 0 \\ 0 \end{bmatrix}, \tag{4}$$

where T_a is the actuation torque provided by the actuator, T_r is the return torque, $\mathbf{I}$ is the 2×2 identity matrix and $\mathbf{0}$ is the null vector. It should be noted that the actuation force F_a is equal to $T_a/r_{a,1}$. Similarly, the return torque is equal to $r_{r,1}F_r$, where F_r is the tension in the return tendon. The transmission factors X_i (where i can be replaced by a or r for actuation and return respectively) depend on the pulley radii and are expressed as:

$$X_{i,2} = \frac{r_{i,3}}{r_{i,1}}, X_{i,3} = \frac{r_{i,5}}{r_{i,1}}. \tag{5}$$

The return torque induced by the return tendon can be computed by the following equation:

$$T_r = -K_r\left(\theta_{a,0} + \mathbf{x}_r^T(\boldsymbol{\theta} - \boldsymbol{\theta}_0)\right), \tag{6}$$

where K_r is the equivalent stiffness of the return tendon mechanism (as seen by the base joint) and $\theta_{a,0} = y_0/r_{r,1}$, y_0 been the difference between the lengths of the tendon after the initial constraint is applied and at rest. The return tendon can be a rigid tendon with a spring attached at its end. The

Jacobian matrix for a three-phalanx robotic finger is defined as:

$$\mathbf{J}^{-T} = \begin{bmatrix} \frac{1}{k_1} & \frac{-\beta_2}{k_1} & \frac{(\beta_2-1)-\psi_3+(\beta_2-1)(\beta_3-1)}{k_1} \\ 0 & \frac{1}{k_2} & \frac{-\beta_3}{k_2} \\ 0 & 0 & \frac{1}{k_3} \end{bmatrix}, \quad (7)$$

where

$$\beta_i = 1 + \frac{l_{i-1}\cos\theta_i}{k_i}, \psi_3 = \frac{l_1\cos(\theta_2+\theta_3)}{k_3}. \quad (8)$$

D. Before Contact

To establish the preshaping motion of the finger before contact, the first step is to compute $\tau_{m,k} = (\tau_{a,k} + \tau_{r,k})$ for every joint. The variable $\tau_{m,k}$ is the equivalent torque at the k^{th} joint induced by the two tendons. The preshaping motion of an underactuated finger is the set of configurations it went through before a contact occurs. The purpose of computing $\tau_{m,k}$ is to establish whether or not a phalanx is blocked by its mechanical limit. If the value is negative, it means the joint is in contact with its particular limit. The first interphalanx joint reaching zero as the input torque T_a increases is the joint that will start to rotate first. The joint will reach its maximal angle if no contact occurs and then, another mechanical limit will stop its motion. Then, as the input torque will increase again, the return torque at another joint will be overcome and its phalanx will begin its rotation. This process continues again a final time for the third and last phalanx.

To make sure the proximal phalanx is the one moving first, a constraint is introduced in the return tendon and the pulleys' diameters are chosen accordingly. After the first phalanx has reached its maximal angle, the second phalanx starts moving followed by the third phalanx. The whole closing sequence is shown in Fig. 3. It should be noted that selecting the mechanical limits at $\pi/2$ is only a design choice. Also, lengths are normalized (dimensionless) throughout the paper. In Fig. 4, the torques due to the mechanical limits are shown using the numerical parameters of Table I. The Jacobian matrix $\mathbf{J}$ been triangular, every element of $\boldsymbol{\tau}$ must be equal to zero until the instant a contact occurs.

Because only one phalanx moves at any time before contact, the closing sequence until the initial contact can be separated in three different stages after the finger starts moving. First, the proximal phalanx rotates around the base joint (initial phase). Then, it reaches its maximum angle limit and the intermediate phalanx starts rotating (intermediate phase). Finally, when the intermediate phalanx hits its own mechanical limit, the distal phalanx starts rotating as the input force in the actuation tendon increases (final phase). The contact can occur during any of these three stages. Therefore, it is critical to analyze the resulting stiffness in all cases.

E. After contact

At the instant of an initial contact, two of the three elements of $\mathbf{f}$ must stay equal to zero. Therefore, one has

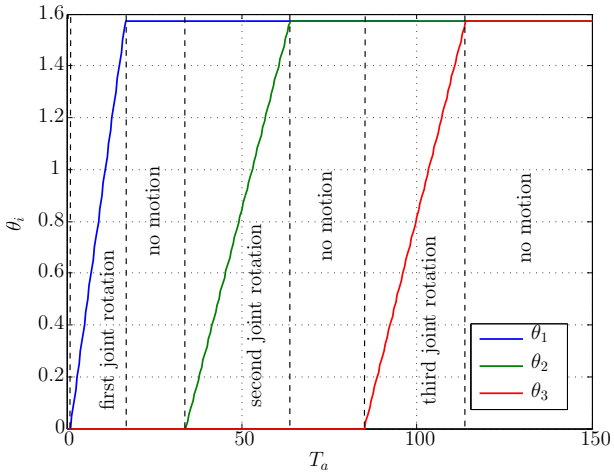

Fig. 3. Joint angles during the preshaping motion

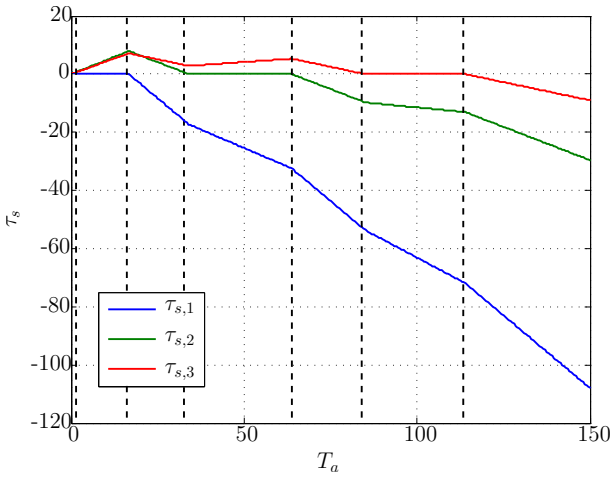

Fig. 4. Torques induced by the mechanical stops at the joints

a system of two equations. Indeed, when there is only one contact with an object, only one element of $\mathbf{f}$ is not equal to zero. Thus, if $\mathbf{J}^{-T}$ is defined as:

$$\mathbf{J}^{-T} = \begin{bmatrix} \mathbf{j}_1 & \mathbf{j}_2 & \cdots & \mathbf{j}_k & \cdots & \mathbf{j}_n \end{bmatrix}^T, \quad (9)$$

then $\mathbf{J}_k^*$ (2×3 matrix) defined for a contact on the k^{th} phalanx can be expressed as:

$$\mathbf{J}_k^* = \begin{bmatrix} \mathbf{j}_1 & \mathbf{j}_2 & \cdots & \mathbf{j}_{k-1} & \mathbf{j}_{k+1} & \cdots & \mathbf{j}_n \end{bmatrix}^T. \quad (10)$$

Considering this definition, one has:

$$\mathbf{J}_k^* \boldsymbol{\tau} = \mathbf{0}. \quad (11)$$

With Eqs. (3-4), the previous equation can be rewritten as:

$$\mathbf{J}_k^* (\mathbf{x}_a T_{a,i} + \mathbf{x}_r T_{r,i} + \boldsymbol{\tau}_{s,i}) = \mathbf{0}. \quad (12)$$

From the general Jacobian matrix, the reduced Jacobian matrices $\mathbf{J}_k^*$ for a 3-DOF finger can be computed for each phalanx:

$$\mathbf{J}_1^* = \begin{bmatrix} 0 & 1 & 0 \\ 0 & 0 & 1 \end{bmatrix}, \tag{13}$$

$$\mathbf{J}_2^* = \begin{bmatrix} 1 & -\beta_2 & 0 \\ 0 & 0 & 1 \end{bmatrix}, \tag{14}$$

$$\mathbf{J}_3^* = \begin{bmatrix} 1 & 0 & -\beta_3 - \psi_3 \\ 0 & 1 & -\beta_3 \end{bmatrix}. \tag{15}$$

In order to have usable $\mathbf{J}_i^*$ matrices, undefined k_i must not be part of the matrix. For example, if a contact occurs on the intermediate phalanx only, k_2 exists but not k_3. In that case, a Gaussian elimination can be used. After contact is made with an object, no motion is possible until at least two joints are not in contact with their mechanical limits. Thus, the input force must increase in order to reach the same torque induced by the contact force and the return tendon. This input increase, ΔT_a, is a function of the contact location. Therefore, by knowing k_i, it is possible to compute ΔT_a (and conversely). First, one has, after contact and until the finger starts moving again:

$$\mathbf{J}_k^*(\mathbf{x}_a(T_{a,i} + \Delta T_a) + \mathbf{x}_r T_{r,i} + \boldsymbol{\tau}_s) = \mathbf{0}. \tag{16}$$

Because the geometrical configuration did not change between this moment and the instant contact began, it is possible to simplify the equation by subtracting Eq. (12):

$$\mathbf{J}_k^*(\mathbf{x}_a \Delta T_a + \boldsymbol{\tau}_s - \boldsymbol{\tau}_{s,i}) = \mathbf{0}. \tag{17}$$

This equation can be rewritten in the following form:

$$\mathbf{J}_k^* \boldsymbol{\tau}_{s,i} = \mathbf{J}_k^* \begin{bmatrix} \mathbf{x}_a & \boldsymbol{\tau}_s \end{bmatrix} \begin{bmatrix} \Delta T_a \\ 1 \end{bmatrix}. \tag{18}$$

As it was noted before, two mechanical limit torques must be equal to zero. Thus, for a three-phalanx finger, only one has a non-zero value. To include this condition in the equation, the vector $\mathbf{s}$ is introduced. This vector is defined by the property that only its k^{th} element is non-zero and equal to 1 where k is the joint that is still locked when motion resumes. Using $\mathbf{s}$ in Eq. (18), it becomes possible to obtain the non-zero mechanical limit torque:

$$\mathbf{J}_k^* \boldsymbol{\tau}_{s,i} = \mathbf{J}_k^* \begin{bmatrix} \mathbf{x}_a & \mathbf{s}\mathbf{s}^T \boldsymbol{\tau}_s \end{bmatrix} \begin{bmatrix} \Delta T_a \\ 1 \end{bmatrix}. \tag{19}$$

Finally, ΔT_a and $\mathbf{s}^T \boldsymbol{\tau}_s$, the remaining mechanical limit torque, can be found with the following equation:

$$\begin{bmatrix} \Delta T_a \\ \mathbf{s}^T \boldsymbol{\tau}_s \end{bmatrix} = \left(\mathbf{J}_k^* \begin{bmatrix} \mathbf{x}_a & \mathbf{s} \end{bmatrix}\right)^{-1} \mathbf{J}_k^* \boldsymbol{\tau}_{s,i}. \tag{20}$$

1) Initial Phase: During the initial phase, only θ_1 increases. Thus, knowing that every interphalanx joint torque must be equal to zero, one can compute $\boldsymbol{\tau}_{si}$ as a function of θ_1 which itself is a function of T_a. Thus, the equation of $\boldsymbol{\tau}_{si}$ is:

$$\boldsymbol{\tau}_{si} = \begin{bmatrix} 0 \\ X_{a,2} - X_{r,2} \\ X_{a,3} - X_{r,3} \end{bmatrix} T_{ai}. \tag{21}$$

An example of the evolution of ΔT_a as a function of the location for a contact occuring during the initial phase is shown in Fig. 5. The proximal phalanx is not shown, because for any value of k_1, the motion afterward (and the value of ΔT_a) is always the same. Only the magnitude of $\mathbf{f}_1$ changes. The proximal phalanx is thus blind from the tactile sensing point of view.

As one can see, although the ΔT_a curve is monotone, which make its possible to detect the contact location from the measured ΔT_a, there is a zone on the second phalanx where the needed torque is the same for any contact location. The two different parts of the curve for a contact occuring on the second phalanx are explained by the fact that two different motions are possible. Before the point b_2, the third interphalanx joint is still locked and the first and second move. After b_2, it is the second joint that is locked, the third joint rotating. Both possibilities are illustrated in Fig. 6. To find out which one corresponds to any k_2, one has to compute the remaining interphalanx mechanical limit torque ($\mathbf{s}^T \boldsymbol{\tau}_s$) and verify if it is negative (meaning there is indeed a contact with the mechanical limit). If it is positive, the other configuration is the valid one. It should be noted that for a joint that is blocked by its opposite limit, the torque has to be positive.

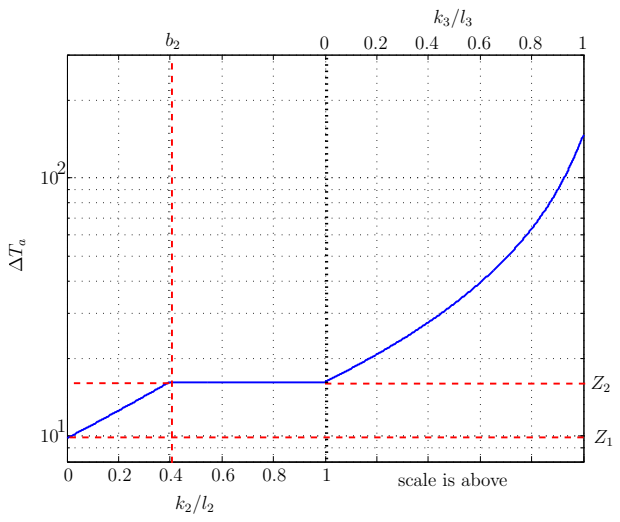

Fig. 5. ΔT_a as a function of the contact location during the initial phase

To better understand Fig. 5, it is important to look at several elements. First, one can compute ΔT_a for a contact at several specific locations. Two of these locations are the interphalanx joints. The values of ΔT_a are defined as the

variables Z_i (shown in Fig. 5). The value of ΔT_a for a contact directly on the second joint (and also for the whole proximal phalanx) can be computed by using Eqs. (13) and (20):

$$Z_1 = -\tau_{si,2}/X_{a,2}. \tag{22}$$

In the case of Z_2, the same thing can be done with Eqs. (14), (20) and $\mathbf{s} = [0\ 1\ 0]^T$ or Eqs. (15), (20), $\mathbf{s} = [0\ 1\ 0]^T$ and $k_3 = 0$:

$$Z_2 = -\tau_{si,3}/X_{a,3}. \tag{23}$$

Finally, b_2 can be computed by taking into account the fact that both possible after-contact motions must be mathematically true at this location. Thus, every element of $\boldsymbol{\tau}_s$ has to be equal to zero. Knowing this, b_2 can be computed from Eq. (19), $\mathbf{J}_2^*$ and Z_2. The simplified equation is:

$$\beta_2(b_2) = \frac{\tau_{si,3} + \tau_{si,1}X_{a,3}}{\tau_{si,2}X_{a,3} - \tau_{si,3}X_{a,2}}. \tag{24}$$

It is interesting to note that $\boldsymbol{\tau}_{si}$ being proportional to T_{ai}, b_2 is thus not a function of T_a but only of the physical parameters of the finger. The complete form of the previous equation is:

$$b_2 = \frac{\tau_{si,2}X_{a,3} - \tau_{si,3}X_{a,2}}{(\tau_{si,1} - \tau_{si,2})X_{a,3} + (1 + X_{a,2})\tau_{si,3}} l_1 \cos\theta_2. \tag{25}$$

It should again be noted that θ_2 being constant during the initial phase, b_2 is also constant.

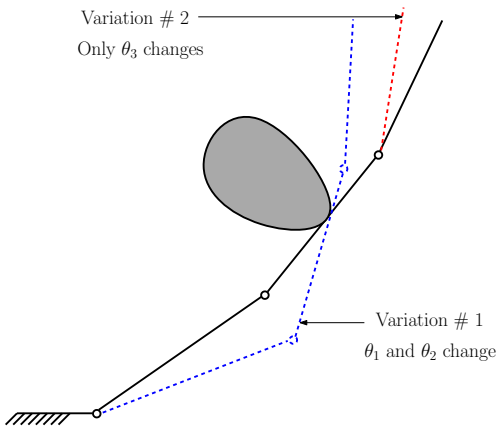

Fig. 6. Possible configurations after motion resumes in the initial phase

2) Intermediate Phase: If the initial contact does not occur during the first stage, the first interphalanx joint reaches its maximum angle and its mechanical limit torque starts increasing. After a certain increase of input torque, the second joint starts rotating (Figs. 3-4). As during the first stage, $\boldsymbol{\tau}_{si}$ can be computed:

$$\boldsymbol{\tau}_{si} = \begin{bmatrix} X_{a,2}/X_{r,2} - 1 \\ 0 \\ X_{a,3} - X_{r,3}X_{a,2}/X_{r,2} \end{bmatrix} T_{ai}. \tag{26}$$

An example of the evolution of ΔT_a is shown in Fig. 7. In this figure, the red vertical plane bounds the intermediate and distal phalanges. It can be observed that for a contact at the beginning of the intermediate phalanx, ΔT_a is equal to zero. It is totally normal, because the first phalanx is already blocked by the mechanical limit. Thus, it is the equivalent of no contact at all.

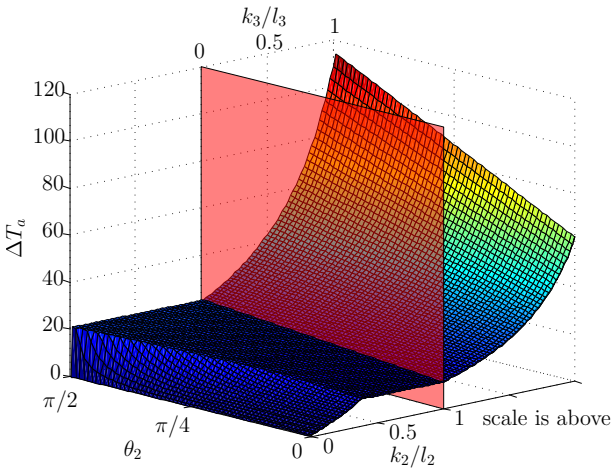

Fig. 7. ΔT_a as a function of the contact location during the intermediate phase

The Z_2 and b_2 equations (Eq. (23) and (25)) are exactly the same as these obtained for the first phase. However, θ_2 varies during this stage and b_2 starts at the same value as the initial phase but it decreases down to zero when θ_2 is equal to $\pi/2$.

3) Final Phase: The final phase, in which the last joint rotates, is easier to analyze, because only contacts on the distal phalanx are possible. As for the other phases, the mechanical limit torques before contact can be computed with this equation:

$$\boldsymbol{\tau}_{si} = \begin{bmatrix} X_{a,3}/X_{r,3} - 1 \\ X_{a,2} - X_{r,2}X_{a,3}/X_{r,3} \\ 0 \end{bmatrix} T_{ai}. \tag{27}$$

In the example illustrated in Fig. 8, it can be seen that ΔT_a increases asymptotically toward infinity. It is explained by the fact that at a certain distance b_3 on the distal phalanx, it is impossible to overcome the return torque by increasing the input torque. This location can be found with Eq. (17) by finding k_3 for which every elements of $\boldsymbol{\tau}_s$ stays the same and do not tend toward zero. Knowing that $\tau_{si,3}$ and $\tau_{s,3}$ are null during this stage, one has:

$$\mathbf{J}_3^* \left(\begin{bmatrix} 1 \\ -X_{a,2} \\ -X_{a,3} \end{bmatrix} \Delta T_a + \begin{bmatrix} \tau_{s,1} \\ \tau_{s,2} \\ 0 \end{bmatrix} - \begin{bmatrix} \tau_{si,1} \\ \tau_{si,2} \\ 0 \end{bmatrix} \right) = \mathbf{0}. \tag{28}$$

By manipulating the variables, two equations can be obtained:

$$\tau_{s,1} = \tau_{si,1} - (1 + X_{a,3}(\beta_3 + \psi_3))\Delta T_a, \tag{29}$$

$$\tau_{s,2} = \tau_{si,2} + (X_{a,2} - \beta_3 X_{a,3})\Delta T_a. \tag{30}$$

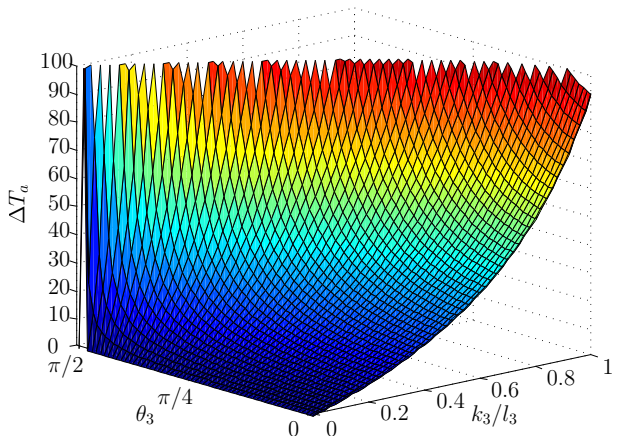

Fig. 8. ΔT_a as a function of the contact location during the final phase

Setting the factor in front of ΔT_a equal to zero, one obtains:

$$b_3 = \frac{X_{a,3} l_2 \cos\theta_3}{X_{a,2} - X_{a,3}}. \tag{31}$$

Beyond b_3, which is a function of θ_3, the finger is completely rigid and no motion is possible. Thus, as the input torque T_a increases, only the contact force magnitude $\mathbf{f}_3$ changes to keep the static equilibrium. It should be noted that the finger is completely rigid no matter the contact location if it occurs on the final phalanx when θ_3 is equal to $\pi/2$.

F. Discussion

As with any theoretical modeling of a physical phenomena, there is always a gap between the simulation results and reality. However, as shown in [9], even if undesired effects such as hysteresis and friction are present, the stiffness variations are typically still measureable. Both contact detection and localization were possible. It also appears reasonable to think that these effects would be less significant in tendon-driven fingers than in compliant linkage-driven fingers as used in [9]. Moreover, the addition of position sensors in the interphalanx joints would also provide redundancy and make it easier to compute the Jacobian matrix in real time. Thus, the relationship between the contact location and the input torque variation is expected to be more robust to noise and other inaccuracies. The geometrical parameters of the finger could also be optimized to reduce the blind zones on the phalanges and improve the precision of the algorithm by increasing the ΔT_a variation. Therefore, many possible avenues exist to improve the algorithm relating the contact location to the input torque variation.

IV. CONCLUSIONS

In this paper, a stiffness analysis of double tendon underactuated fingers was presented. It was followed by numerical simulations providing new insights on the effect of several design parameters on the finger stiffness. From the previous analysis, it can be demontrated that a contact localization algorithm can be obtained from Eq. (20). Future work will center on the application of this method on an experimental prototype.

ACKNOWLEDGMENT

The support of the National Science and Engineering Research Council (NSERC) is gratefully acknowledged as well as the *Fonds de recherche du Quebec - Nature et Technologies*, the Canadian Foundation for Innovation and the *Ingenierie de technologies interactives en readaptation* (INTER).

REFERENCES

[1] S. Hirose and Y. Umetani, "Development of soft gripper for the versatile robot hand," *Mechanism and Machine Theory*,vol. 13(3), pp. 351–359, 1978.

[2] M. Carrozza, *et al.*, "The SPRING hand: Development of a self-adaptive prosthesis for restoring natural grasping," *Autonomous Robots*, vol. 16(2), pp. 125–141, 2004.

[3] M. Baril, T. Laliberte, C.M. Gosselin, and F. Routhier, "On the design of mechanically programmable underactuated anthropomorphic robotic and prosthetic grippers," in *Proc. ASME International Design Engineering Technical Conferences and Computers and Information in Engineering Conference (IDETC/CIE'12)*, vol. 5(A), Chicago, IL, Aug. 2012, pp. 85–95.

[4] R. Ozawa, K. Hashirii, Y. Yoshimura, M. Moriya, and H. Kobayashi, "Design and control of a three-fingered tendon-driven robotic hand with active and passive tendons," *Autonomous Robots*, DOI: 10.1007/s10514-013-9362-z, pp. 1–12, 2013.

[5] Y.-L. Park, K. Chau, R.J. Black, and M.R. Cutkosky, "Force sensing robot fingers using embedded fiber bragg grating sensors and shape deposition manufacturing," in *Proc. IEEE International Conference on Robotics and Automation (ICRA'07)*, Roma, Italy, April 2007, pp. 1510–1516.

[6] V. Duchaine, N. Lauzier, M. Baril, M.-A. Lacasse, and C.M. Gosselin, "A flexible robot skin for safe physical human robot interaction," in *Proc. IEEE International Conference on Robotics and Automation (ICRA'09)*, Kobe, Japan, May 2009, pp. 3676–3681.

[7] A. Bicchi, J. Salisbury, and P. Dario, "Augmentation of grasp robustness using intrinsic tactile sensing," in *Proc. IEEE International Conference on Robotics and Automation (ICRA'89)*, vol. 1, Scottsdale, AZ, May 1989, pp. 302–307.

[8] D. Simpson, *The control of upper-extremety prostheses and orthoses*, C.C. Thomas, 1974, *The choice of control system for the multimovement prosthesis: Extended physiological proprioception*, 1974, pp. 146–150.

[9] B. Belzile and L. Birglen, "A compliant self-adaptive gripper with proprioceptive haptic feedback," *Autonomous Robots*, DOI: 10.1007/s10514-013-9360-1, pp. 1–13, 2013.

[10] S.B. Backus and A.M. Dollar, "Robust, inexpensive resonant frequency based contact detection for robotic manipulators," in *Proc. IEEE International Conference on Robotics and Automation (ICRA'12)*, Saint Paul, MN, May 2012, pp. 1514–1519.

[11] M. Kaneko and K. Tanie, "Contact point detection for graspingof an unknown object using self-posture changeability (spc)," in *Proc. IEEE International Conference on Robotics and Automation (ICRA'90)*, Cincinnati, OH, May 1990, pp. 864–869.

[12] G.S. Koonjul, G.J. Zeglin, and N.S. Pollard, "Measuring contact points form displacements with a compliant articulated robot hand," in *Proc. IEEE International Conference on Robotics and Automation (ICRA'11)*, Shanghai, China, May 2011, pp. 489–495.

[13] M. Ciocarlie and P. Allen, "A design and analysis tool for underactuated compliant hands," in *Proc. IEEE/RSJ International Conference on Intelligent Robots and Systems (IROS'09)*, St. Louis, MO, Oct. 2009, pp. 5234–5239.

[14] F. Guay and C. Gosselin, "Static model for a 3-dof underactuated finger," in *Mechanical Sciences*, vol. 2, pp. 65–71, 2011.

[15] L. Birglen, T. Laliberte, and C. Gosselin, *Underactuated Robotic Hands*, B. Siciliano, O. Khatib, and F. Groen, Eds. Springer Tracts in Advanced Robotics, 2008.